Petroleum and Coal

Article **Open Access**

Textural Characteristics and Depositional Environment of the Permian Sandstones of the Ecca Group in Borehole KWV-1: Evidence from Grain Size Analysis

Mahlatse M Ntake, Ronaldo Malapana, Tsibula J Sekantsi, Sibusiso Maseko, Mokgadi K Teffo and Christopher Baiyegunhi*

Department of Geology and Mining, University of Limpopo, Private Bag X1106, Sovenga 0727, Limpopo Province, South Africa

Received May 23, 2023; Accepted July 20, 2023

Abstract

Grain size analysis is a vital sedimentological tool used to unravel the hydrodynamic conditions, mode of transportation and deposition process of detrital sediments. Despite the distinct stratigraphic sequence and lithological variation of the Ecca Group in the southern Main Karoo Basin, up to now, there is not much information on the grain size parameters of the sandstones. In addition, the few measured statistical parameters were not adequately related to the mode of transportation and deposition. As a result, a total of 35 sandstones from borehole KWV-1 were investigated for their grain size distributions. To unravel the transportation mechanisms, textural characteristics and depositional environment of the sandstones, grain size statistical parameters, binary plots, linear discriminant plots and Passega diagrams were used. The grain size parameters indicated that the sandstones were fine-grained to very fine-grained and displayed near symmetrical patterns. The binary plots indicate that these samples were deposited mostly by wind (aeolian action) with a few deposited by other transportation mediums. From the Visher diagram, it is evident that the main transportation mode is saltation with a few sediments in suspension and traction. The Passega diagrams unravelled that there were fluctuations in energy levels, thus indicating that the samples were transported through rolling and suspension, saltation and graded suspension. According to the linear discriminant plots (LDF), the investigated sandstones are turbidity currents sediments. Furthermore, the LDF disclosed that the sedimentation process of the Collingham, Ripon and Fort Brown Formations occurred in shallow marine environments. Prince Albert deposits are indicated to be lacustrine-deltaic. These samples are further proven to have been deposited by tractive currents.

Keywords*: Grain size analysis; Textural parameters; Depositional environment; Sandstones.*

1. Introduction

Clastic sedimentary rocks have distinctive textural characteristics that may be put to various uses. Grain size is one of the most important descriptive aspects of sediments frequently used in geology. Grain sizes are analysed to derive the depositional environment of sediments, the depositional processes, transport mechanisms, and energy of the transport medium during sedimentation [1]. The distribution, percentages, maturity, sorting of grains have an impact on soil and rock qualities [2]. Grain size analysis is one of the main descriptive methods employed to analyse textural characteristics of clastic sedimentary rocks. It is defined as a descriptive textural characterization method used in the measurement of unconsolidated sediments sizes, to reveal their depositional environment, depositional processes and their hydrodynamic conditions [3-4].

Grain size analysis is primarily focused on measuring and categorising the grain size and graphically using this data for various purposes. The measured grain sizes are plotted on cumulative frequency curves which give data for the calculation of statistical parameters including; mean, standard deviation, kurtosis and skewness. Several researchers including [5-7] have denoted that sediments deposited under different environmental conditions differ in terms of their grain sizes, colour, sedimentary structures and other textural characteristics. This implies that sediments reflect any environmental change that occurred throughout their deposition and lithification into rocks. Studying these sediments may therefore give out their source material, transportation and depositional processes [2]. Textural parameters such as the grain's roundedness, minerals and biogenic components can be used to further substantiate and give out the depositional environment and the transportation medium's energy during deposition [3,7].

Karoo Basins are situated in various southern African countries such as Swaziland, Zambia, Zimbabwe, Botswana, Malawi, South Africa, Congo, Angola and Tanzania. The total area of these basins is about 4 500 000 km^2 with the southern part of the main basin estimated to be 12 km thick [8]. South Africa hosts a major sedimentary basin known as the Main Karoo Basin which consists of rock suites deposited under varying conditions. The rock strata and sediments are said to have originated from the underlying Cape Supergroup as well as the Namaqua Natal Metamorphic Belt [9]. The Karoo Supergroup is predominantly comprised of sedimentary rocks as well as economically viable ores such as coal which are mainly in the Ecca Group.

The area under study is situated in the Eastern Cape Province of South Africa within the vicinity of the Willowvale area, in the Mbashe local municipality (Figure 1).This study is based on determining the depositional environment and transportation mechanisms of sandstones in Borehole KWV-1 through grain size analysis.

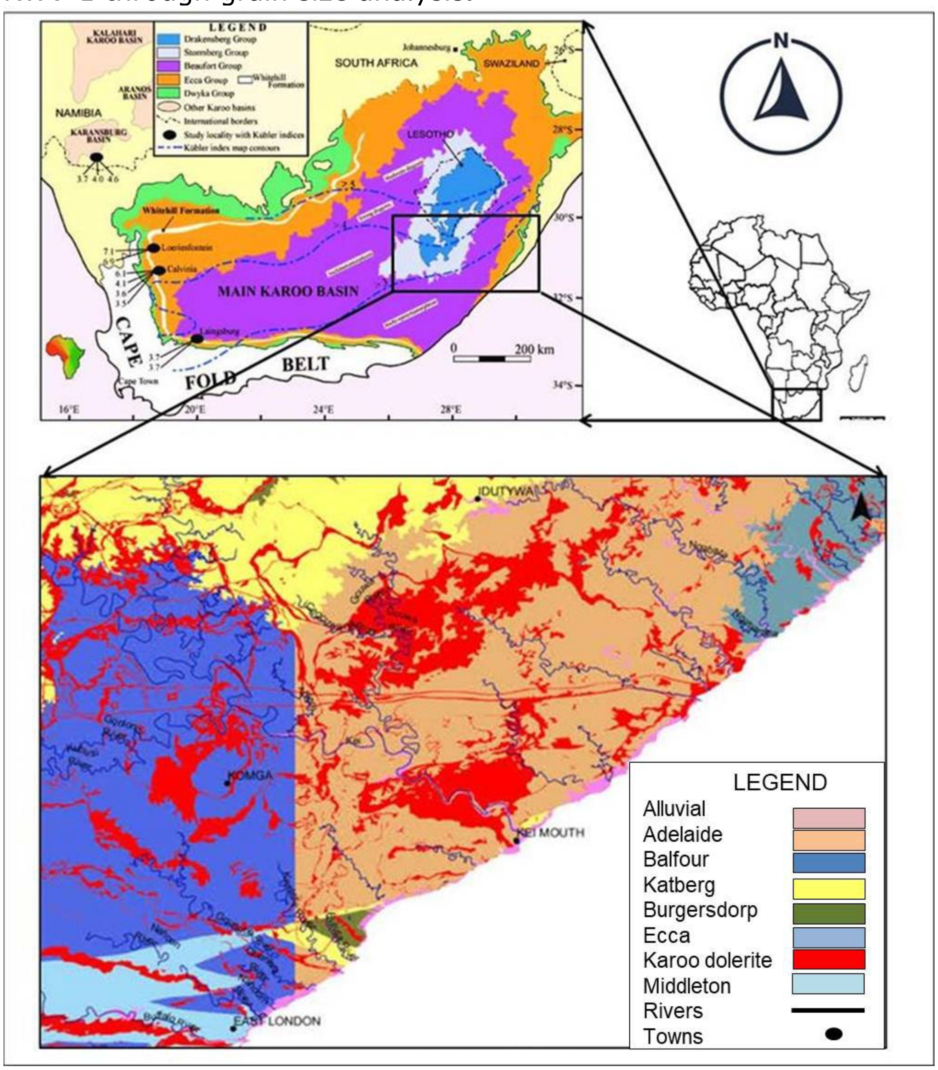

Figure 1. Geological map showing the location of borehole KWV-1 around the Willowvale area in the Eastern Cape Province, South Africa (modified after [10])

2. Geological setting

"Karoo" is a term which was invented as a description of the sedimentary fill of basins which are comparable in age across all Gondwana [3-4]. Sedimentation in these intra-cratonic basins commenced in the Late Carboniferous (300 Ma) and concluded in the Middle Jurassic (183 Ma), representing over 100 Ma of continuous sedimentation [10-13]. The Main Karoo Basin covers about two thirds of South Africa with an area of about 700 000 km^2 [3,10]. When compared to other Gondwana basins, it has a complete stratigraphic sequence which is also very thick [14]. Karoo lithologies were laid in two margins of Gondwana, in the northern and southern margin. In the north, these rocks lie unconformably on the Archaean basement and in the south, they were laid conformably on the Proterozoic Namaqua-Natal Metamorphic Belt [9,15-16]. The northern part of this basin is much thinner than the southern part (Figure 2).

There are various models developed to describe the geology and tectonic setting of the Karoo Supergroup. However, the most widely used model to date, is the one suggesting that the Karoo Supergroup was initiated in the north-western margin of the Gondwana Supercontinent, and the sediments were deposited in a retro-arc large foreland basin [9,17-19]. According to [18,20-21] an ongoing orogeny and compression triggered the formation of the then 6000 km long Cape Fold Belt in the southern margin of Gondwana. Studies conducted by [18,22] further suggested that the infilling of the sediments was mainly controlled by subsidence and the orogenic loading and unloading in the basin. The subsidence was severe around the Cape Fold Belt in the south and some crustal thickening is also evident in this area. The northern margin experienced some thinning as compared to the southern margin, furthermore, it was suggested that one of the main attributes in the sequences of the foreland basin is the thickening of the crust towards the orogeny [23].

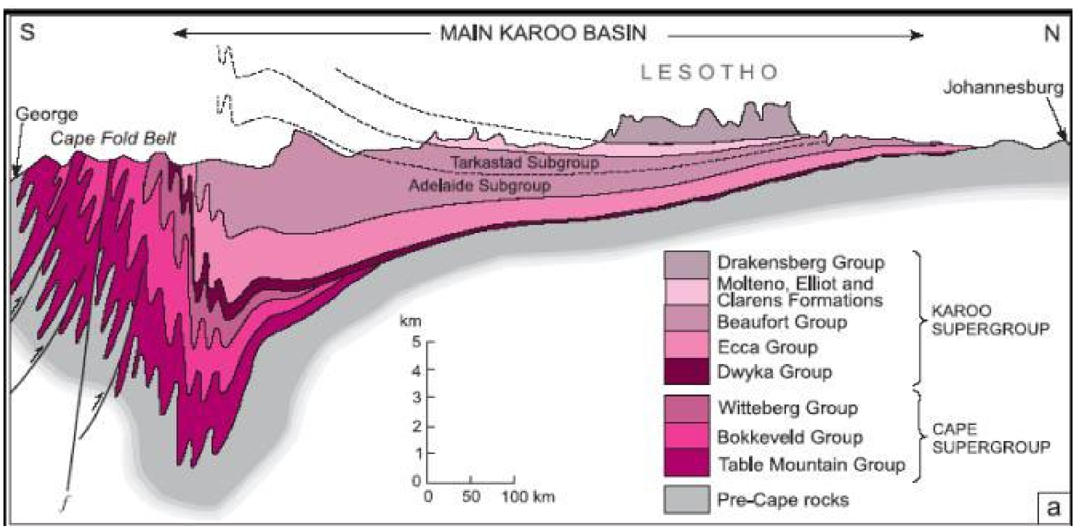

Figure 2. The foreland basin model of the Karoo Basin exhibiting a southern crustal thickening and a northern crustal thinning [23]

Five stratigraphic groups make up the Karoo Supergroup, namely; Dwyka, Ecca, Beaufort, Stormberg and the Drakensburg Groups [9,15]. According to [9], these groups were deposited in glacial, deep marine, deltaic, fluvial and aeolian (under true desert conditions) environments. The first deposits were in glacial environments and these incorporate the Dwyka sediments. This was followed by deep marine conditions in which the lower Ecca Group sediments were deposited. The overlying Beaufort and Stormberg Groups were deposited in deltaic to fluvial and aeolian conditions, respectively. Sedimentation was halted by the extrusive lavas during the deposition of Drakensburg Group, in the Mid Jurassic era, when Gondwana Supercontinent was breaking up [11,18]. This study was conducted on samples obtained from the Ecca Group of the Karoo Supergroup.

3. Materials and methods

The main lithologies in borehole KWV-1 were identified through core logging, thereafter, the logged core was sampled for sandstones. From the samples, thin sections were prepared for petrographic studies and grain size analysis. This analysis entailed examining and conventionally measuring the longest axis of the grains on photomicrographs [24-25]. At least 400 grains were counted and measured in each photomicrograph and the grain size frequencies were classified as per the Udden-Wentworth grade scale [26-27]. The measured dimensions in millimetres were then converted to a logarithmic phi scale by applying the following formula: $\Phi = -\log_2 D$; where, Φ is the phi size and D is the diameter of the grain in millimetres (mm).

Cumulative frequency curves and frequency histograms were then derived using the results obtained from the grain size analyses. From the cumulative frequency curves, various percentile values in phi were graphically derived (Figure 3). These percentile values were then used to develop statistical data with the aid of mathematical expressions in order to determine the sorting and other textural characteristics of each sample. Various equations by [28] were then used to calculate the grain size distributions from the statistical parameters (Table 1).

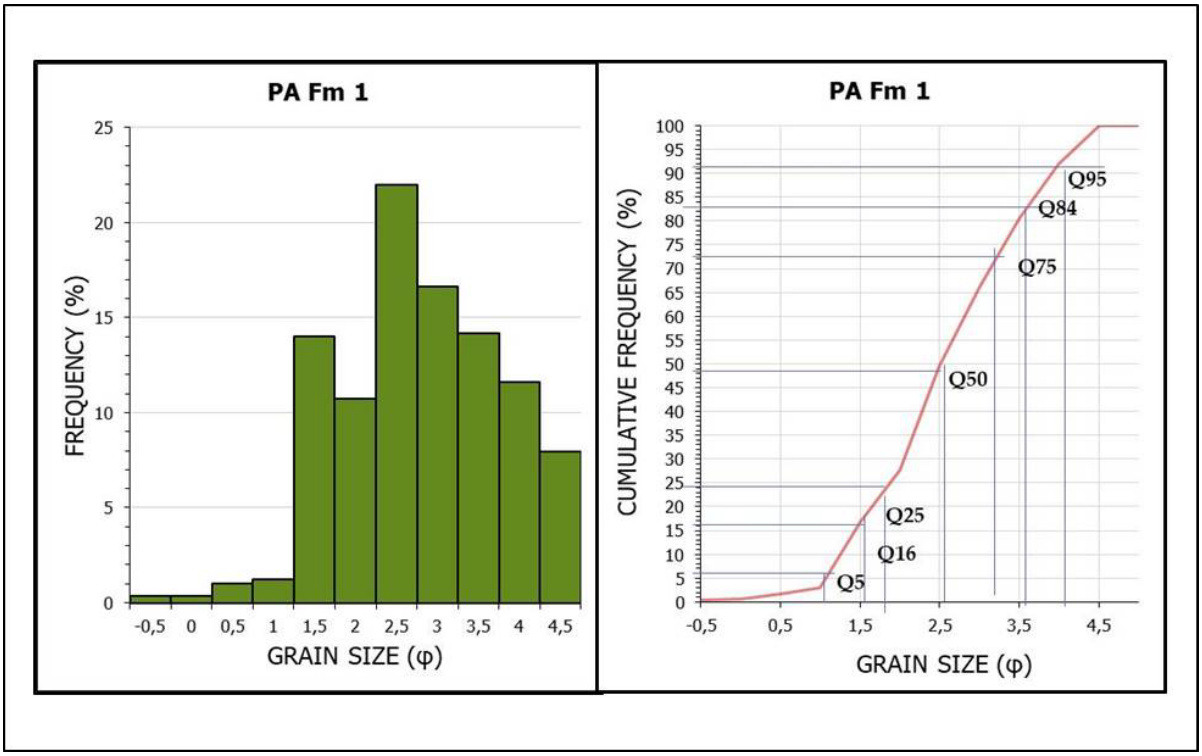

Figure 3. Cumulative frequency curve (left) and the frequency histograms (right) for Prince Albert Formation sample 1 (labelled PA Fm 1)

Table 1. Formulas for deriving statistical parameters using graphically derived data [28]

Grain size parameter	Formula
Mean (Mz)	$M_z = \frac{\emptyset_{16} + \emptyset_{50} + \emptyset_{84}}{3}$
Standard deviation (σi)	$\sigma i = \frac{\emptyset_{84} - \emptyset_{16}}{4} + \frac{\emptyset_{95} - \emptyset_5}{6.6}$
Skewness (SKi)	$SKi = \frac{\emptyset_{84} + \emptyset_{16} - 2\emptyset_{50}}{2(\emptyset_{84} - \emptyset_{16})} + \frac{\emptyset_{95} + \emptyset_5 - 2\emptyset_{50}}{2(\emptyset_{95} - \emptyset_5)}$
Kurtosis (K_G)	$K_G = \frac{(\emptyset_{95} - \emptyset_5)}{2.44(\emptyset_{75} - \emptyset_{25})}$

The 5th, 16th, 25th, 50th, 75th, 84th and 95th percentile values are represented by Φ_5, φ_{16}, φ_{25}, φ_{50}, φ_{75}, φ_{84} and φ_{95} on the cumulative curves, respectively.

The parameters used are the standard deviation, mean, skewness and the kurtosis (Table 1). According to [1], each statistical parameter is defined as follows:

3.1. Mean (M_z)

The mean is defined as a variable used to describe the general size of the grains for samples. It is therefore the average of all the measured sizes of the grains in a certain sample. The average size or the mean is used to give the central tendency of the distributed grains using the formulas shown in Table 1.

3.2. Standard deviation (σ_i)

The sorting of the grains in a certain sample measured by the standard deviation. This parameter describes how the grains vary and how they are distributed based on their sizes and compares that with the overall size of the grains. The formula in Table 1 is used to calculate the standard deviation values and these values are then used to give the degree of sorting in a particular sample using Table 2.

Table 2. Verbal sorting corresponding to different phi standard deviation values [29]

Standard deviation values in phi	Verbal sorting
<0.35	Very well sorted
0.35 to 0.50	Well sorted
0.50 to 0.70	Moderately well sorted
0.70 to 1.00	Moderately sorted
1.00 to 2.00	Poorly sorted
2.00 to 4.00	Very poorly sorted
>4.00	Extremely poorly sorted

3.3. Skewness (SK_i)

In order to give the symmetry of the grain size distributions, skewness is calculated using the formula in Table 1. This is a statistical parameter describing most of the measured grain sizes, the further the value is from 0, the more skewed the sample is as shown by Table 3.

Table 3. Verbal skewness matching with the calculated phi skewness values [29]

Skewness values in phi	Verbal skewness
> 0.30	Strongly fine skewed
0.30 to 0.10	Fine skewed
0.10 to -0.10	Near symmetrical
-0.10 to -0.30	Coarse skewed
<-0.30	Strongly coarse skewed

3.4.Kurtosis (K_G)

Kurtosis is defined as a descriptive parameter which gives the sharpness of a frequency curve of grain sizes through a comparison of spread of the tails in the centre of the curve to those at the end. The verbal kurtosis is given in Table 4.

Table 4. Verbal kurtosis for a certain range of a calculated phi kurtosis values [29]

Kurtosis values in phi	Verbal kurtosis
<0.67	Very platykurtic
0.67 to 0.90	Platykurtic
0.90 to 1.11	Mesokurtic
1.11 to 1.50	Leptokurtic
1.50 to 3.00	Very leptokurtic
>3.00	Extremely leptokurtic

4. Results

4.1. Stratigraphy

The total depth of borehole KWV-1 is 2352.39 m and it incorporates dolerite intrusions as well as sediments of the Koonap Formation, the Ecca Group and the Dwyka Group (Figure 4). Prince Albert, Whitehill, Collingham, Fort Brown and the Ripon Formations make up the Ecca Group in borehole KWV-1.

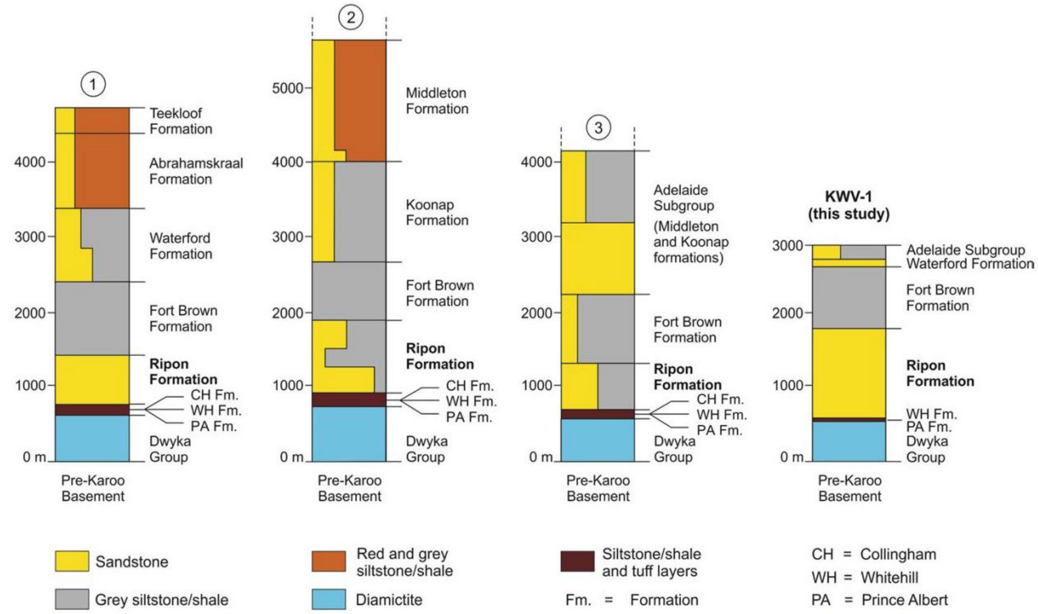

Figure 4. Stratigraphic column of borehole KWV-1 displaying the Permian Ecca Group (Prince Albert, Collingham, Ripon and Fort Brown Formations) and the Beaufort Group (Middleton, Koonap, Abrahamsgraal and Teekloop Formations), after [20].

4.2. Petrography

The sandstones in borehole KWV-1 were observed under the microscope for petrographic analysis. The samples from the Ecca Group are dominated by quartz (Figure 5).

4.3. Textural characteristics

The textural characteristics of the sandstone samples from the Ecca Group are displayed in Table 5.

Table 5. Textural characteristics of the sandstones from the Ecca Group

Formation	Sample ID	Grain Size	Verbal grain size	Roundness	Sorting
Prince Albert	PA Fm 1	2.55	Fine sand	Sub-angular	Poorly sorted
	PA Fm 2	2.20	Fine sand	Sub-angular	Poorly sorted
	PA Fm 3	2.50	Fine sand	Angular	Poorly sorted
	PA Fm 4	2.48	Fine sand	Sun-angular	Poorly sorted
	PA Fm 5	2.68	Fine sand	Sub-angular	Poorly sorted
Collingham	CH Fm 1	2.82	Fine sand	Sub-rounded	Moderately well sorted
	CH Fm 2	3.11	Very fine sand	Rounded	Well sorted
	CH Fm 3	3.33	Very fine sand	Sub-angular	Moderately well sorted
	CH Fm 4	3.27	Very fine sand	Sub-rounded	Moderately well sorted
	CH Fm 5	3.12	Very fine sand	Sub-rounded	Moderately well sorted
Ripon	R Fm 1	2.40	Fine sand	Sub-rounded	Well sorted
	R Fm 11	2.77	Fine sand	Sub-angular	Well sorted
	R Fm 5	2.95	Fine sand	Rounded	Well sorted
	R Fm C	3.11	Very fine sand	Sub-rounded	Moderately well sorted
	R Fm 8	2.93	Fine sand	Sub-rounded	Well sorted
	R Fm P	3.17	Very fine sand	Rounded	Moderately well sorted

Formation	Sample ID	Grain Size	Verbal grain size	Roundness	Sorting
Ripon	R Fm 2	2.03	Fine sand	Sub-rounded	Well sorted
	ZN02L	2.92	Fine sand	Sub-rounded	Well sorted
	R Fm 3	2.27	Fine sand	Sub-rounded	Well sorted
	ZN02K	2.44	Fine sand	Sub-rounded	Well sorted
	R Fm 1A	2.08	Fine sand	Rounded	Moderately well sorted
	R Fm 9	2.47	Fine sand	Sub-rounded	Well sorted
	R Fm 2A	2.56	Fine sand	Sub-angular	Well sorted
	R Fm 6	2.96	Fine sand	Sub-angular	Very well sorted
	R Fm 4	3.00	Very fine sand	Sub-angular	Very well sorted
	R Fm 7	3.12	Very fine sand	Rounded	Well sorted
	R Fm 5A	2.88	Fine sand	Sub-rounded	Well sorted
	R Fm B	2.38	Fine sand	Sub-rounded	Well sorted
	R Fm 10	3.05	Very fine sand	Sub-angular	Well sorted
Fort Brown	FB Fm 1	2.13	Fine sand	Rounded	Well sorted
	FB Fm 2	3.07	Very fine sand	Sub-rounded	Moderately well sorted
	FB Fm 3	2.02	Fine sand	Sub-angular	Moderately well sorted
	FB Fm 4	2.17	Fine sand	Sub-rounded	Well sorted
	FB Fm 5	2.03	Fine sand	Rounded	Moderately well sorted
	FB Fm 6	2.47	Fine sand	Sub-rounded	Well sorted

4.4. Grain size statistics

The graphic percentile phi values were graphically derived from the cumulative frequency curves. The results are displayed by Table 6.

Table 6. The graphic percentile values of the analysed samples from the Ecca Group

Sample ID	Φ_1	Φ_5	Φ_{16}	Φ_{25}	Φ_{50}	Φ_{75}	Φ_{84}	Φ_{95}	C(μm)	M(μm)
PA Fm 1	0.19	1.07	1.48	1.88	2.51	3.31	3.66	4.19	877	176
PA Fm 2	-0.10	0.65	1.21	1.48	2.12	2.82	3.28	3.98	1047.5	230
PA Fm 3	0.01	0.98	1.50	1.80	2.32	3.27	3.69	4.14	993	200
PA Fm 4	-0.31	1.01	1.41	1.75	2.43	3.26	3.60	4.14	1245	186
PA Fm 5	-0.39	0.96	1.70	1.97	2.56	3.50	3.79	4.23	1310	170
CH Fm 1	2.00	2.08	2.30	2.47	2.80	3.19	3.37	3.79	250	144
CH Fm 2	2.04	2.27	2.61	2.78	3.14	3.43	3.57	3.97	243	113
CH Fm 3	2.03	2.35	2.79	3.03	3.31	3.70	3.89	4.28	245	101
CH Fm 4	2.11	2.53	2.74	2.90	3.21	3.50	3.87	4.30	232	108
CH Fm 5	2.05	2.29	2.60	2.74	3.09	3.44	3.68	4.07	241	117
R Fm 1	1.52	1.64	1.93	2.09	2.40	2.75	2.88	3.17	348	189
R Fm 11	1.45	2.03	2.27	2.48	2.79	3.11	3.25	3.43	372	145
R Fm 5	2.02	2.32	2.58	2.69	2.94	3.23	3.33	3.47	247	130
R Fm C	1.39	1.82	2.55	2.70	3.10	3.47	3.69	4.00	382	117
R Fm 8	2.02	2.18	2.53	2.63	2.91	3.22	3.35	3.50	248	133
R Fm P	1.90	2.29	2.66	2.83	3.18	3.47	3.67	3.98	268	110
R Fm 2	1.03	1.28	1.60	1.73	2.07	2.33	2.43	2.72	490	238
ZN02L	2.01	2.17	2.53	2.63	2.91	3.20	3.32	3.44	249	136
R Fm 3	1.10	1.52	1.79	2.02	2.27	2.55	2.76	3.08	470	207
ZN02K	1.35	1.62	2.05	2.14	2.40	2.73	2.86	3.14	400	187
R Fm 1A	1.01	1.20	1.58	1.73	2.11	2.41	2.55	2.93	497	232
R Fm 9	1.53	1.70	2.04	2.15	2.45	2.79	2.91	3.24	346	183
R Fm 2A	1.57	1.97	2.15	2.28	2.60	2.85	2.93	3.24	337	165
R Fm 6	2.11	2.51	2.62	2.70	2.94	3.22	3.32	3.44	232	130
R Fm 4	2.10	2.40	2.62	2.73	3.03	3.27	3.36	3.47	238	122
R Fm 7	2.00	2.38	2.65	2.80	3.14	3.42	3.58	3.93	250	113
R Fm 5A	2.02	2.15	2.50	2.59	2.85	3.15	3.28	3.44	246	139
R Fm B	1.10	1.46	2.03	2.11	2.34	2.63	2.78	2.97	470	198
R Fm 10	2.03	2.22	2.59	2.73	3.09	3.36	3.46	3.80	245	117
FB Fm 1	1.04	1.43	1.67	1.80	2.14	2.42	2.58	2.88	485	227
FB Fm 2	1.91	2.12	2.52	2.67	3.08	3.43	3.60	3.87	266	118
FB Fm 3	1.00	1.15	1.53	1.68	2.04	2.38	2.49	2.91	500	243
FB Fm 4	1.40	1.51	1.69	1.84	2.17	2.46	2.66	3.02	380	222
FB Fm 5	0.90	1.17	1.58	1.71	2.04	2.36	2.47	2.85	523	243
FB Fm 6	1.03	1.52	1.98	2.12	2.50	2.82	2.93	3.30	490	177

The one percentile value in microns is represented by C and M is the median value in microns.

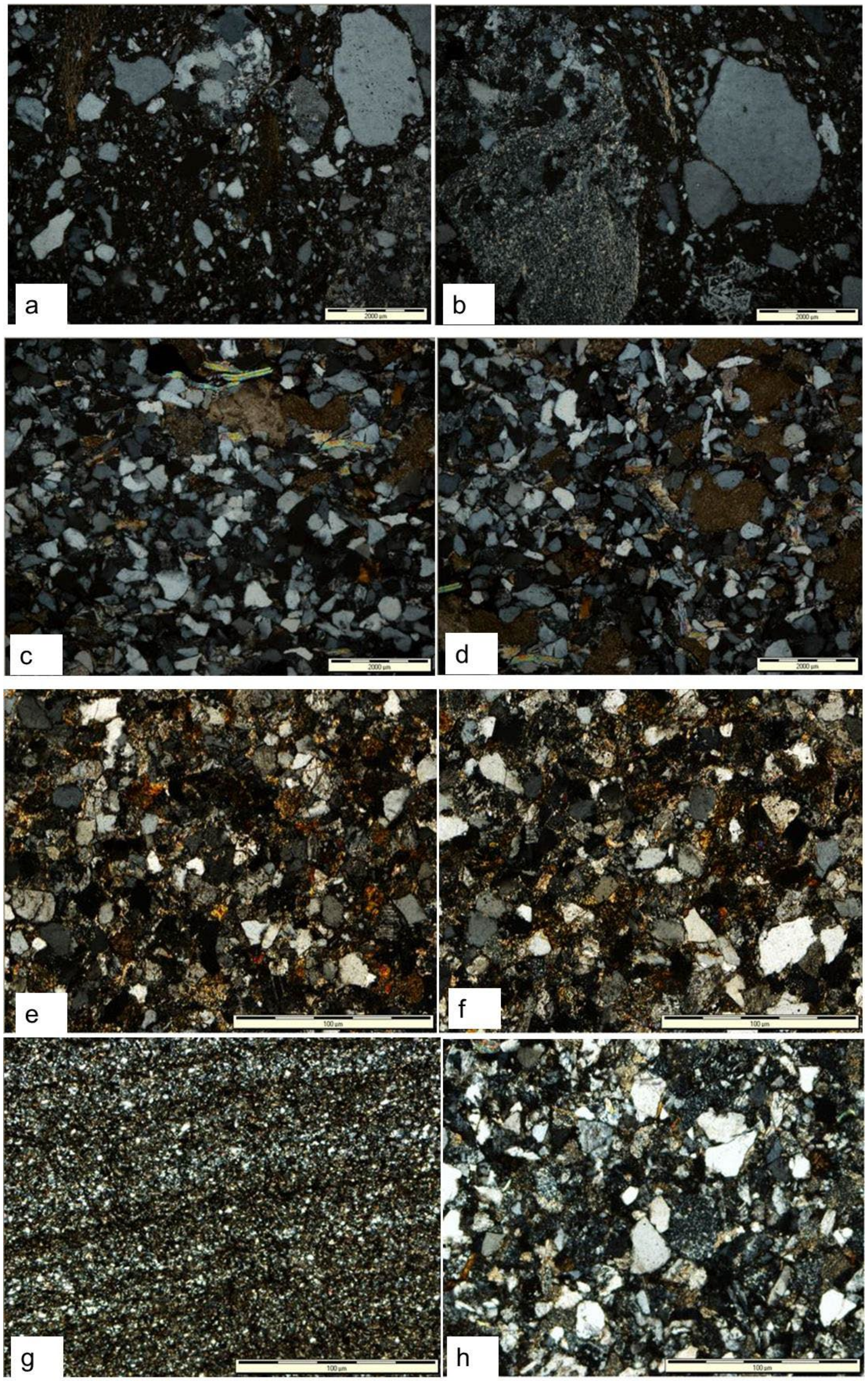

Figure 5. Photomicrographs depicting: (a) Poorly sorted sandstones of Prince Albert; (b) Sub-angular fine grained sandstones of the Prince Albert Formation; (c) Moderately sorted grains and fine grained sandstones (d) of the Collingham Formation; (e) Fine grained sandstones of Ripon Formation; (f) Sub-angular sandstones of the Ripon Formation; (g) Very fine grained and moderately well sorted grains (h) of the Fort Brown Formation

5. Interpretations and discussion

5.1. Stratigraphy

Borehole KWV-1 encompasses lithologies from the Prince Albert, Collingham, Ripon and Fort Brown Formations (Figure 4). It also contains rocks from the Adelaide Subgroup, Waterford Formation and the Dwyka Group. The base of this borehole is dominated by diamictites of the Dwyka Group. This is overlain by the sandstones of the Ripon, Prince Albert and Whitehill Formations which have been intruded by dolerite in places. The overlying Fort Brown Formation is comprised of a mixture of fine sediments, that is, silt and shale which is greyish in colour. Sandstones and interlayers of silts and shales make up the overlying Waterford Formation and Adelaide Subgroup, respectively.

5.2. Petrography

The Permian sandstones of the Ecca Group are dominated by quartz minerals, followed by feldspars (Figure 5). However, minute amounts of other minerals such as calcite and hematite can be observed. Within all the samples, the dominating mineral is quartz which is about 20-30% in composition. Most of the quartz minerals are sub-angular and generally fine grained. The second most plentiful mineral in the sandstones is feldspar with composition ranging between 15-25%. There is twinning and it can be observed on the sub-rounded to sub-angular shaped feldspar minerals. The minerals are within some matrix and cement with the most abundant cement being the clay, feldspar, calcite and quartz.

5.3. Grain size statistical parameters

The graphic mean, inclusive graphic standard deviation, kurtosis and skewness were calculated based on the equations by [28]. The results of these parameters are displayed and interpreted by Table 7 and Figure 6.

5.3.1. Mean (M_z)

The average size (in phi) of the grains which are examined is calculated using the mean. This parameter also gives the overall conditions in terms of energy during the deposition of the sample. The average sizes of the particles in Prince Albert Formation fall between 2.20 and 2.68 phi. Additionally, average sizes of the Collingham, Ripon and Fort Brown Formations range from 2.82 to 3.33, 2.03 to 3.17 and 2.02 to 3.07 phi, respectively (Table 7). Prince Albert Formation contained only fine grained samples whilst very fine grained sandstones dominate the Collingham Formation. The Fort Brown and Ripon Formations predominantly consists of fine grained particles. The variation in size indicate that the depositional energy varies, however, the lack of coarse grained particles within the samples and the dominance in fine grained particles show that the energy during deposition was generally low [1]. This is comparable with a study by [4] for the sandstones in the Bredasdorp Basin whereby the variation in sizes was associated with unstable energy as deposition occurred.

5.3.2. Standard deviation (σ_I)

The overall consistency of the sizes of the grains or the uniformity of the grains is derived from the standard deviation value. According to [30], this parameter also reflects the hydrodynamic energy in a certain environment. Prince Albert samples are poorly sorted with their standard deviation phi values ranging from 1.01 to 1.02. The phi standard deviation numerical values of samples from CH Fm are between 0.49 and 0.59. These are in correspondence to moderately well sorted and well sorted sediments. The well sorted to moderately well sorted grains of the Ripon Formation have a calculated standard deviation value between 0.30 and 0.57. The Fort Brown Formation samples are moderately well sorted with minute number of well sorted samples and their values are between 0.47 and 0.54. Studies carried out by [31-32] indicate that moderately well sorted patterns displayed by some grains may be owed to the removal of those grains by air current or/ and the introduction of earlier sorted sediments in marine environments.

5.3.3. Skewness (SK_i)

This parameter shows how spread the grains are in a sample on the basis of grain size distributions. The skewness of a distribution curve is categorised as symmetrical or asymmetrical based on their shaped. The asymmetrical graphs with more coarse grained particles have negative kurtosis values whilst those dominated by fine grains have positive numerical values. All the samples from PA Fm are near symmetrical except for one with the values between 0.05 and 0.17. The other formations are near symmetrical and their values range from -0.06 to 0.11, -0.09 to 0.07 and -0.07 to 0.03 for Collingham, Ripon and Fort Brown Formations, respectively. The near-symmetrical pattern of the curves agrees with the notion that there were no utmost conditions like the variation in tides [4,33].

5.3.4. Kurtosis (K_G)

The sharpness of a graph is reflected by the calculated kurtosis phi values. If a graph is sharply peaked, then it means that the middle part of the distribution curves for the grains is better sorted than the tails; the opposite is true for flat peaked graphs. Prince Albert Formation has the kurtosis values between 0.85 and 1.02 and the curves are all platykurtic except for one. The kurtosis values of the Collingham Formation are in between 0.97 and 1.21 phi and the curves are leptokurtic to mesokurtic. Ripon Formation has a variety of curves which are mesokurtic, leptokurtic and platykurtic with the values between 0.73 and 1.20. All curves of the Fort Brown Formation are mesokurtic with values between 0.94 and 1.06. The sandstones in this group are mostly mature and this is displayed by the dominance of platykurtic to mesokurtic grains as well as the roundness of these grains. This may be as a result of dominance of fine grained sandstones and the low energy amid deposition [32].

Table 7. The calculated grain size parameters and their verbal interpretation

Sample ID	M_z	σ_i	SK_i	K_G	Interpretation
PA Fm 1	2.55	1.02	0.05	0.89	Fine grained ,poorly sorted, platykurtic, near symmetrical
PA Fm 2	2.20	1.02	0.10	1.02	Fine grained, poorly sorted, mesokurtic, near symmetrical
PA Fm 3	2.50	1.03	0.17	0.88	Fine grained, poorly sorted, platykurtic, fine skewed
PA Fm 4	2.48	1.02	0.06	0.85	Fine grained ,poorly sorted, platykurtic, near symmetrical
PA Fm 5	2.68	1.02	0.10	0.88	Fine grained ,poorly sorted, platykurtic, near symmetrical
CH Fm 1	2.82	0.53	0.06	0.97	Fine grained, moderately well sorted, mesokurtic, near symmetrical
CH Fm 2	3.11	0.49	-0.06	1.07	Very fine grained, well sorted, mesokurtic, near symmetrical
CH Fm 3	3.33	0.57	0.03	1.18	Very fine grained, well sorted, leptokurtic, near symmetrical
CH Fm 4	3.27	0.55	0.11	1.21	Very fine grained, well sorted, leptokurtic, near symmetrical
CH Fm 5	3.12	0.54	0.06	1.04	Very fine grained, well sorted, leptokurtic, near symmetrical
R Fm 1	2.40	0.47	0.01	0.95	Fine grained, well sorted, mesokurtic, near symmetrical
R Fm 11	2.77	0.46	-0.04	0.91	Fine grained, well sorted, mesokurtic, near symmetrical
R Fm 5	2.95	0.36	0.01	0.87	Fine grained, well sorted, platykurtic, near symmetrical
R Fm C	3.11	0.62	-0.02	1.16	Very fine grained, moderately well sorted, leptokurtic, near symmetrical
R Fm 8	2.93	0.41	0.02	0.92	Fine grained, well sorted, mesokurtic, near symmetrical
R Fm P	3.17	0.51	-0.02	1.08	Very fine grained, moderately well sorted, mesokurtic, near symmetrical
R Fm 2	2.03	0.43	-0.08	0.99	Fine grained, well sorted, mesokurtic, near symmetrical
ZN02L	2.92	0.39	0.01	0.91	Fine grained, well sorted, mesokurtic, near symmetrical
R Fm 3	2.27	0.48	0.01	1.21	Fine grained, well sorted, leptokurtic, near symmetrical
ZN02K	2.44	0.43	0.07	1.06	Fine grained, well sorted, mesokurtic, near symmetrical
R Fm 1A	2.08	0.51	-0.06	1.04	Fine grained, moderately well sorted, mesokurtic, near symmetrical
R Fm 9	2.47	0.45	0.03	0.99	Fine grained, well sorted, mesokurtic, near symmetrical
R Fm 2A	2.56	0.39	-0.08	0.91	Fine grained, well sorted, mesokurtic, near symmetrical
R Fm 6	2.96	0.32	0.05	0.73	Fine grained, well sorted, mesokurtic, near symmetrical
R Fm 4	3.00	0.35	-0.07	0.81	Fine grained, very well sorted, mesokurtic, near symmetrical
R Fm 7	3.12	0.47	-0.02	1.03	Very fine grained, well sorted, mesokurtic, near symmetrical
R Fm 5A	2.88	0.39	0.04	0.94	Fine grained, well sorted, mesokurtic, near symmetrical
R Fm B	2.38	0.42	0.06	1.19	Fine grained, well sorted, mesokurtic, near symmetrical
R Fm 10	3.05	0.46	-0.09	1.03	Fine grained, well sorted, leptokurtic, near symmetrical
FB Fm 1	2.13	0.45	-0.01	0.96	Fine grained, well sorted, mesokurtic, near symmetrical
FB Fm 2	3.07	0.54	-0.03	0.95	Very fine grained, moderately well sorted, mesokurtic, near symmetrical
FB Fm 3	2.02	0.51	-0.03	1.03	Fine grained, moderately well sorted, mesokurtic, near symmetrical
FB Fm 4	2.17	0.47	0.03	1.00	Fine grained, well sorted, mesokurtic, near symmetrical
FB Fm 5	2.03	0.48	-0.02	1.06	Fine grained, well sorted, mesokurtic, near symmetrical
FB Fm 6	2.47	0.51	-0.07	1.04	Fine grained, well sorted, mesokurtic, near symmetrical

where Mz, σ_I, SK_i and K_G are a representation of the mean, standard deviation, skewness and kurtosis values in phi, respectively.

Figure 6. Statistical textural parameters of the Ecca Group sandstones

5.4. Bivariate plots of the textural parameters

Two textural parameters can be combined to construct binary plots which give off the depositional environments of the sediments. The basis for bivariate plots is the presumption that the statistical variables or parameters accurately reveal the discrepancies in the fluid flow mechanisms for the transportation and deposition of sediments [3]. These plots have been demonstrated and verified by numerous researchers [28,34-35] to be the effective methods for determining the various sedimentation environments. Additionally, it has been noted that these plots are the most crucial and widely utilized plots [28,36].

5.4.1. Standard deviation versus mean

This plot compares the sorting (standard deviation) and the average grain size (Figure 7). The grain sizes of well sorted sediments amid prolonged transportation prior to deposition is generally the same or similar. According to [37], the difference in grain size implies that the sediments' source is close or quick sediment deposition. The majority of the examined sandstones are either fine grained or very fine grained. This may be due to prolonged transportation to the depositional environment. Furthermore, these grains may have collided with other features or with other grains enroute to deposition. Prince Albert Formation is said to be a deep marine sediments and sandstones within shales and mudstones. This group is dominated by poorly sorted grains and this may be due to short transportation distance as the sediments were perhaps deposited closer to their source. A study by [3] suggests that there was an ongoing reworking of sediments in Collingham, Ripon and Fort Brown Formations by current; the substantial amounts of well sorted to moderately well sorted grains in these formations agree with this suggestion.

5.4.2. Skewness versus mean

The binary plot of skewness against mean was used to determine the depositional processes of the sandstones in the Ecca Group using the combined bivariate plots boundaries (Figure 8). This bivariate plot contains three borders which contain various processes of deposition, that is, deposition by aeolian action, wave action and the river [36,38-39]. This diagram illustrates that the sediments derived from Prince Albert were deposited via an aeolian action. Samples from the other formations were mostly deposited by an aeolian action, with a few sandstones from the Ripon Formation deposited by the either the wave or the river. Although most samples fall within those three borders, other samples do not fall within those three borders. This may be due to the fact that there are other depositional processes that are not included by this plot and the unclassified samples may have been deposited by other depositional processes. Studies by [3-4] indicated that the sandstones show an inverted V-shaped curve and this agrees with the near symmetrical nature of the sandstone samples used in this study.

5.4.3. Kurtosis versus skewness

The analysed samples were mostly mesokurtic, with a few samples being either leptokurtic or platykurtic (Figure 7). Prince Albert Formation contains samples which are platykurtic with an exception of one analysed sample which is mesokurtic. Three samples from the Collingham Formation were mesokurtic whilst two of the analysed samples were leptokurtic. Most of the samples from the Ripon Formation are mesokurtic with a few samples being either leptokurtic or platykurtic. Fort Brown Formation contains samples which are mesokurtic. The dominance of samples in the mesokurtic region shows that the samples contain grain sizes which are widely distributed. Tremendously low or high kurtosis values entail that the sediments underwent high energy conditions to achieve their sorting [39].

5.4.4. Skewness versus standard deviation

The bivariate chart of skewness against the sorting (standard deviation) displays that almost all the samples are near symmetrical, however, sample PA Fm 3 from is finely skewed (Figure 7). The sediments are all moderately well-sorted to well-sorted excluding the poorly sorted sandstones in the basal formation. The near symmetrical character of the sandstones may be a consequence of the deficiency in additional energy from exterior transportation mechanism such as variation in currents and depositional actions [4]. Furthermore, it may indicate that there was no major change in the slope which may have resulted in additional of energy and detritus material.

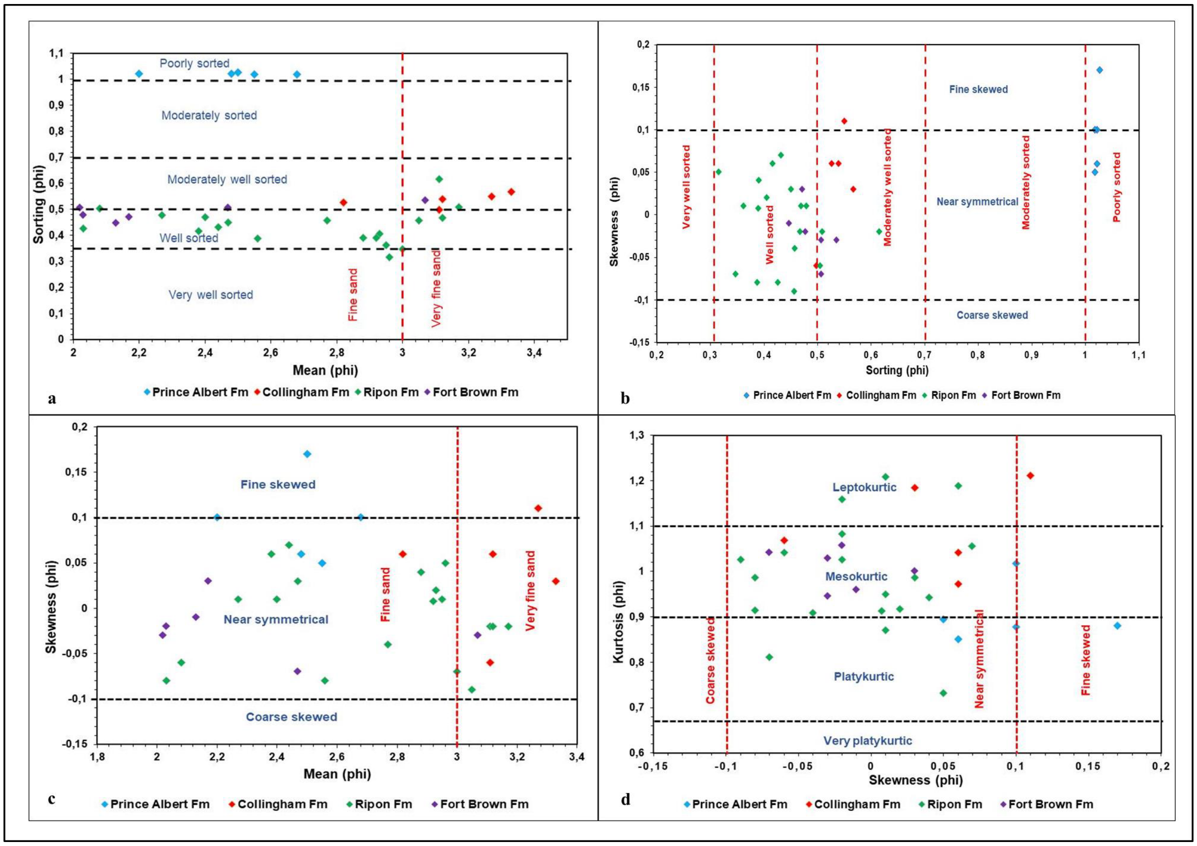

Figure 7. (a) Binary plots of sorting against mean; (b) Binary plot of skewness against sorting; (c) Binary plot of skewness against mean; (d) Binary plot of kurtosis against skewness

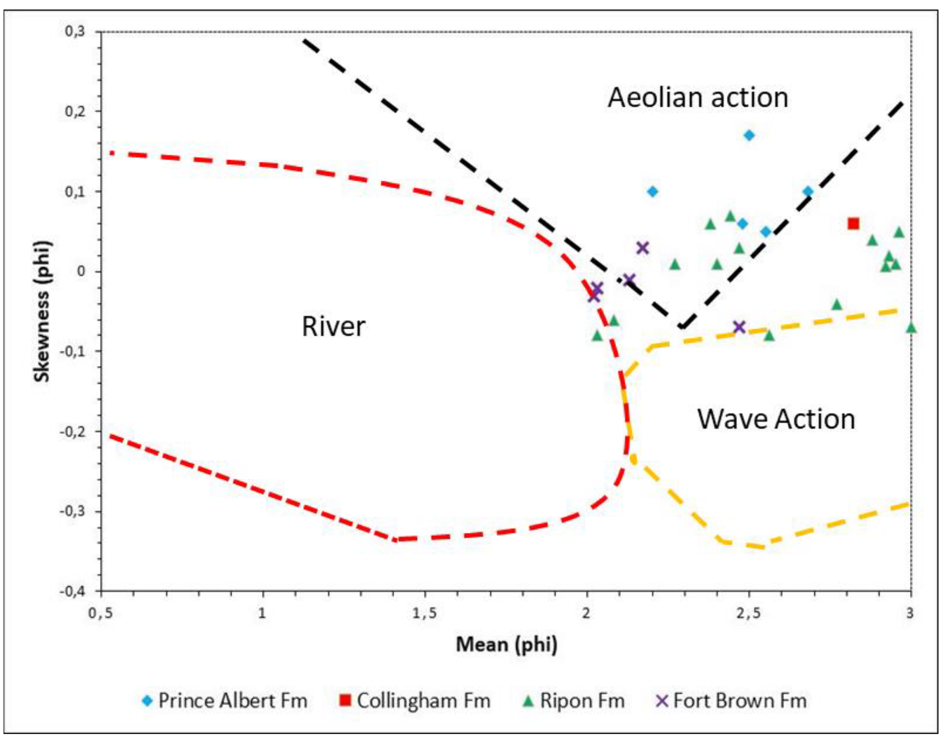

Figure 8. Binary plot of mean against skewness which shows various depositional processes for the sampled sandstones (boundaries after [36,38-39])

5.5. Visher diagrams

The transportation mechanisms of the Ecca Group sandstones were denoted by log probability curves which were developed by Visher [40]. The diagram uses three transportation mechanisms, namely, traction, saltation and suspension. Traction transportation mechanism involves movement of large boulders and rocks which are rolled along a river bed. Stones and small pebbles move through bouncing along the bed of a river via saltation whilst suspension involves the movement of very light and fine sediments which are moved by water. Prince Albert Formation is predominantly made up of sediments which were transported through saltation (about 80%), with several sediments transported by traction (25%) and a minute amount (about 5%) of sediments transported by suspension (Figure 9). Furthermore, about 85% of the sediments of the Collingham Formation were transported via saltation with a few sediments carried in suspension. There are only two transportation mechanisms used in the Ripon Formation, which are, saltation (90%) and suspension (5%), with saltation being the dominant transport mechanism (Figure 9). The Fort Brown Formation indicates that the sediments were mostly transported through saltation (75%) and the others were transported by traction (about 3%) and approximately 15% through suspension (Figure 9).

When compared to the fine grained suspension sediments, the saltation sediments are substantially more sorted whilst the traction reflects a smaller number of poorly sorted sediments. Internal forces which are producing the sliding or rolling movements could be the cause of the dominating saltation populations which are between 1.5 phi and 2.5 phi [40] in [3]. Prince Albert shows breaks which are not as abrupt as the other formations; this may be the results of the mixing of debris brought by currents which are varying in energies and distinct in provenances [41]. As noted by [40], the log curves displayed are similar to well-known trends for historical river deposits.

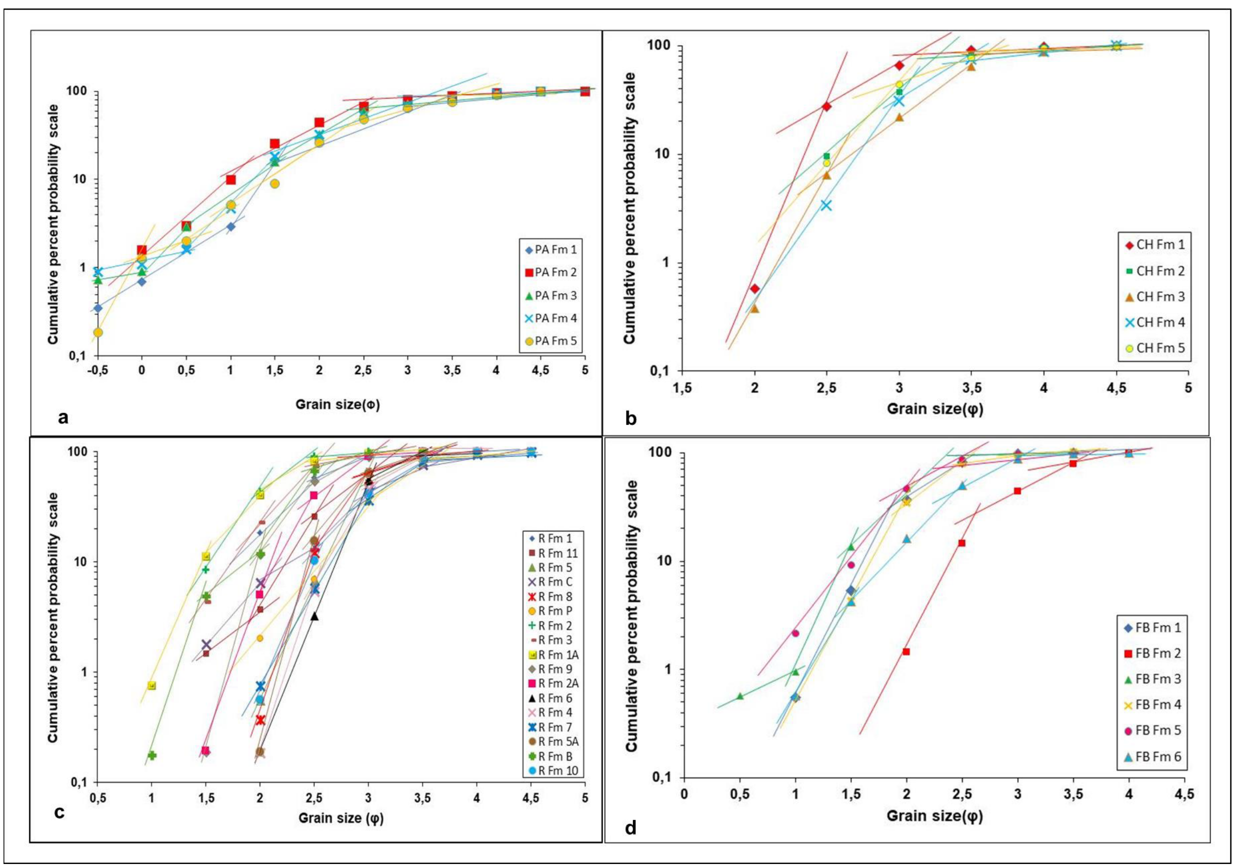

Figure 9. Arithmetic log probability curves revealing various transportation mechanisms in: (a)Prince Albert Formation; (b) Collingham Formation; (c) Ripon Formation; (d); Fort Brown Formation (after [40])

5.6. Passega diagrams (C-M pattern)

A binary plot of C versus M was instigated by [42] in order to depict hydrodynamic forces which are in place amid the deposition of sediments. The C-M plot is a binary log against log probability scale diagram plotted using C (i.e., the one percentile (coarsest materials) values in microns) and M (i.e., the median values in microns) as depicted by Table 6. The C and M were chosen because according to [43], the coarse sediment fraction (represented by C) is much more reliable in representing the sedimentation agent than finer grained sediments. The nature of the hydrodynamic forces as per the Passega diagrams relates to the transportation medium energy as described by Visher diagrams [40,43]. There are several forces depicted by the C-M plot, namely, rolling and suspension (OP), rolling (NO), suspension and rolling (PQ), graded suspension which is mostly suspension (QR), uniform suspension (RS) and pelagic suspension (T). These hydrodynamic forces correlate to different conditions of transport and deposition in the marine and littoral settings.

The sandstone samples from the basal formation (i.e., Prince Albert) fall within the OP region meaning that they were transported through rolling and suspension (Figure 10). In the QR region (the saltation region), there are samples from the overlying Collingham Formation. All the other analysed sediments from both the Fort Brown and Ripon Formations fall within the QR (graded suspension) and the PQ (suspension and rolling) region. If the value of the C value increases, it means that there is a change in the energy level [44]. This clearly shows that energy level increases with the increase in the C values because in order to move coarser grained materials, more energy is required. Another C-M plot was developed to denote the depositional environment of the sandstones [42]. These depositional environments are classified as tills, river-terrace gravel, pelagic, beach, tractive current and beach gravel. The C-M plot for all the analysed samples displays that they were deposited by tractive currents (Figure 11). The CM pattern for the Ecca Group sandstones and the trend is the same as the one used by [3]. In addition, a study by [44] also shows a similar trend for the sandstones in the Stormberg Group.

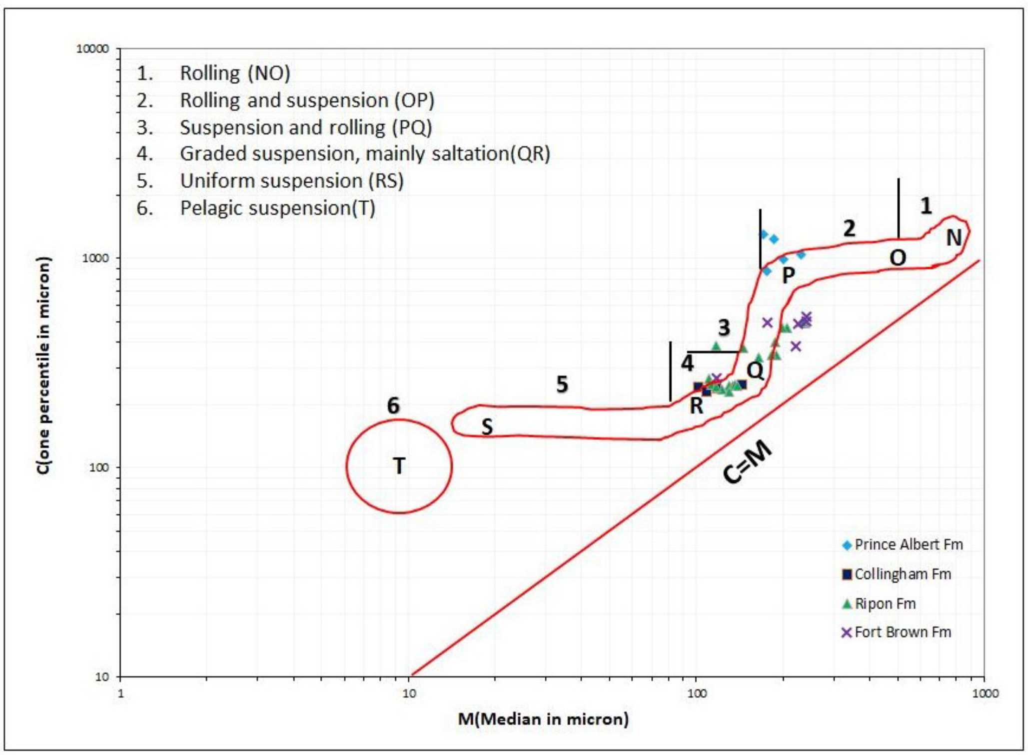

Figure 10. C-M plot displaying the transportation mechanisms for the analysed sandstones (after [42])

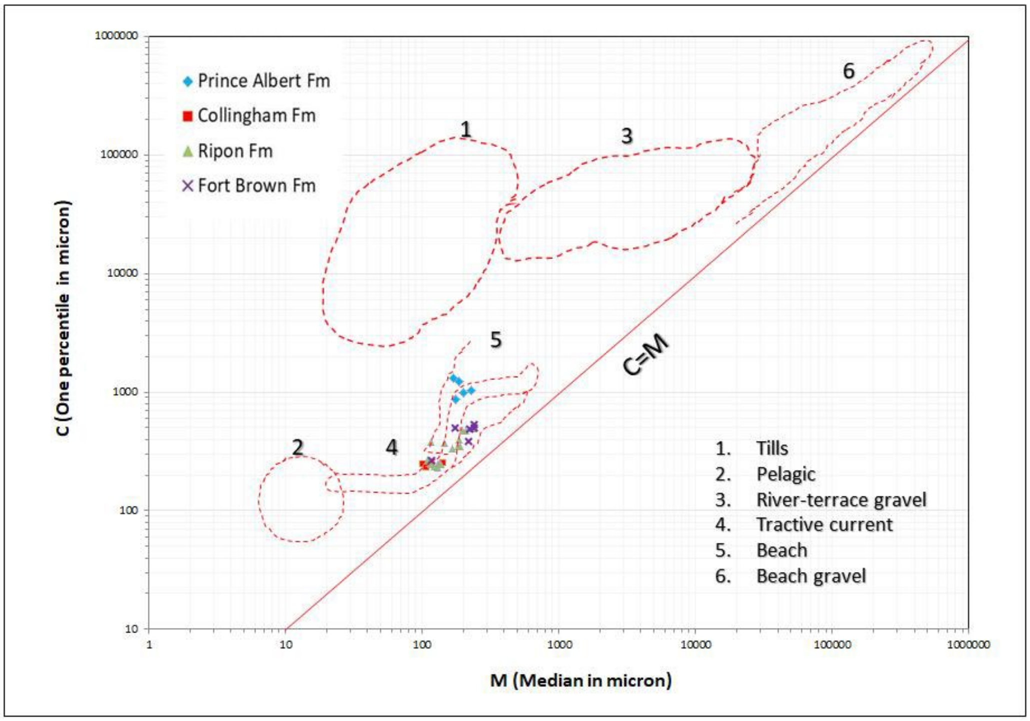

Figure 11. C-M plot indicating the environment of deposition for the analysed sandstone samples (after [42])

5.7. Linear Discriminate Functions (LDF)

The linear discriminant functions (LDF) were developed by [30] to show varying depositional environments. These are Y1 which differentiates the beach and shallow agitated water environment, Y2 which classify sediments into either shallow marine or beach, Y3 which is either deltaic / and lacustrine or shallow marine, and Y4 which categorise sediments as turbidity or deltaic. The Sahu linear discriminant functions were developed for the sediments from Ecca Group using the following equations [30]:

$Y1_{\text{(Shallow A; B)}} = -3.5688M + 3.7016r^2 - 2.0766SK + 3.1135KG$ (1)

Sediments are from the shallow agitated water and beach if Y1 is < -2.7411 and Y1 is>-2.7411, respectively. The environments may be classified as either beach or shallow marine using equation 2.

$Y2_{\text{(B; SM)}} = 15.6534M + 65.7091r^2 + 18.1071SK + 18.5043KG$ (2)

Sediments belong to the beach if Y2< -65.3650 and they belong to the shallow marine if Y2> -65.3650. To differentiate deltaic (lacustrine) environments from shallow marine environments, equation 3 was used:

$Y3_{\text{(SM, F)}} = 0.2852M - 8.7604r2 - 4.8932SSK + 0.0482KG$ (3)

A Y3 value > -7.4190 classify sediments as shallow marine and Y3< -7.4190 classifies sediments as deltaic (lacustrine). Sediments were further classified as deltaic and turbidity current deposits using equation 4 below:

$Y4_{\text{(F; T)}} = 0.7215M - 0.4030r^2 + 6.7322SK + 5.2927KG$ (4)

A Y4 value is <9.8433 shows turbidity current and Y4> 9.8433 reflects deltaic deposits. From the equations the mean, the standard deviation, skewness and kurtosis values are represented by M, r, SK and KG respectively. The analysed samples were calculated and the values are displayed by Table 8.

Table 8. Calculated linear discriminant values with the corresponding depositional environments for the sediments of the Ecca Group [30]

Sample ID	LDF VALUE				ENVIRONMENTS			
	Y1	Y2	Y3	Y4	Y1	Y2	Y3	Y4
PA Fm 1	-6.90	83.67	-1.42	7.32	Shallow A	Shallow M	Shallow M	Turbidity
PA Fm 2	-3.10	67.83	-1.49	8.06	Shallow A	Shallow M	Shallow M	Turbidity
PA Fm 3	-3.73	69.74	-1.32	8.03	Shallow A	Shallow M	Shallow M	Turbidity
PA Fm 4	-3.17	66.15	-1.51	7.11	Shallow A	Shallow M	Shallow M	Turbidity
PA Fm 5	-4.41	75.45	-1.47	7.66	Shallow A	Shallow M	Shallow M	Turbidity
CH Fm 1	-6.14	81.44	-1.87	7.69	Shallow A	Shallow M	Shallow M	Turbidity
CH Fm 2	-6.73	83.65	-0.94	7.59	Shallow A	Shallow M	Shallow M	Turbidity
CH Fm 3	-7.07	95.73	-1.96	9.00	Shallow A	Shallow M	Shallow M	Turbidity
CH Fm 4	-7.00	95.53	-2.20	9.63	Shallow A	Shallow M	Shallow M	Turbidity
CH Fm 5	-6.94	88.33	-1.91	8.28	Shallow A	Shallow M	Shallow M	Turbidity
R Fm 1	-4.81	69.80	-1.25	6.91	Shallow A	Shallow M	Shallow M	Turbidity
R Fm 11	-6.20	73.19	-0.80	6.62	Shallow A	Shallow M	Shallow M	Turbidity
R Fm 5	-7.35	71.07	-0.31	6.85	Shallow A	Shallow M	Shallow M	Turbidity
R Fm C	-6.05	94.65	-2.27	8.39	Shallow A	Shallow M	Shallow M	Turbidity
R Fm 8	-7.04	73.97	-0.65	7.16	Shallow A	Shallow M	Shallow M	Turbidity
R Fm P	-6.94	86.30	-1.21	7.98	Shallow A	Shallow M	Shallow M	Turbidity
R Fm 2	-3.34	60.48	-0.57	6.21	Shallow A	Shallow M	Shallow M	Turbidity
ZN02L	-7.03	72.70	-0.49	7.04	Shallow A	Shallow M	Shallow M	Turbidity
R Fm 3	-3.51	73.16	-1.35	8.19	Shallow A	Shallow M	Shallow M	Turbidity
ZN02K	-4.86	71.18	-1.23	7.89	Shallow A	Shallow M	Shallow M	Turbidity
R Fm 1A	-3.11	67.49	-1.29	6.71	Shallow A	Shallow M	Shallow M	Turbidity
R Fm 9	-5.05	70.82	-1.18	7.28	Shallow A	Shallow M	Shallow M	Turbidity
R Fm 2A	-5.57	65.40	-0.14	6.20	Shallow A	Shallow M	Shallow M	Turbidity
R Fm 6	-8.02	67.34	-0.20	6.38	Shallow A	Shallow M	Shallow M	Turbidity
R Fm 4	-7.59	68.62	-0.18	6.03	Shallow A	Shallow M	Shallow M	Turbidity
R Fm 7	-7.09	81.81	-0.80	7.63	Shallow A	Shallow M	Shallow M	Turbidity
R Fm 5A	-6.86	73.26	-0.66	7.39	Shallow A	Shallow M	Shallow M	Turbidity
R Fm B	-4.27	71.73	-1.07	8.48	Shallow A	Shallow M	Shallow M	Turbidity
R Fm 10	-6.73	78.82	-0.40	7.10	Shallow A	Shallow M	Shallow M	Turbidity
FB Fm 1	-3.85	133.54	-8.23	6.75	Shallow A	Shallow M	Deltaic/Lacustrine	Deltaic
FB Fm 2	-3.49	125.53	-8.57	10.47	Beach	Shallow M	Deltaic/Lacustrine	Deltaic
FB Fm 3	-1.05	124.31	-9.10	10.93	Beach	Shallow M	Deltaic/Lacustrine	Deltaic
FB Fm 4	-2.60	129.09	-9.48	12.57	Beach	Shallow M	Deltaic/Lacustrine	Deltaic
FB Fm 5	-2.54	125.30	-8.57	11.85	Shallow A	Shallow M	Deltaic/Lacustrine	Deltaic
FB Fm 6	-3.31	128.05	-8.67	12.19	Shallow A	Shallow M	Deltaic/Lacustrine	Turbidity

where, shallow M and shallow A represent the shallow marine and the shallow agitated water environments, respectively.

The LDF of Y2 against Y1 indicates that the analysed sandstones are all from shallow agitated water or aeolian environment with an exception of samples (FB Fm 2 to FB Fm 4) which fall under the beach environment (Figure 12). The Y3 versus Y2 linear discriminant function suggests that examined sediments from Prince Albert, Collingham and Ripon Formations are shallow marine deposits. This plot additionally shows that the Fort Brown Formation sandstones were deposited in lacustrine or deltaic environments (Figure 13). The calculated Y2 numerical values indicate that the sandstones are all shallow marine deposits. The Y4 against Y3 linear discriminant function (Figure 14) depicts that the analysed sandstones from Fort Brown Formation were deposited by turbidity currents or deltaic processes. It further shows that the samples from the other formations (Prince Albert, Collingham and Ripon) were deposited by turbidity currents or shallow marine deposits. This agrees with a study by [4] which classified the Ecca Group sandstones as being deposited by turbidity currents in shallow marine environments.

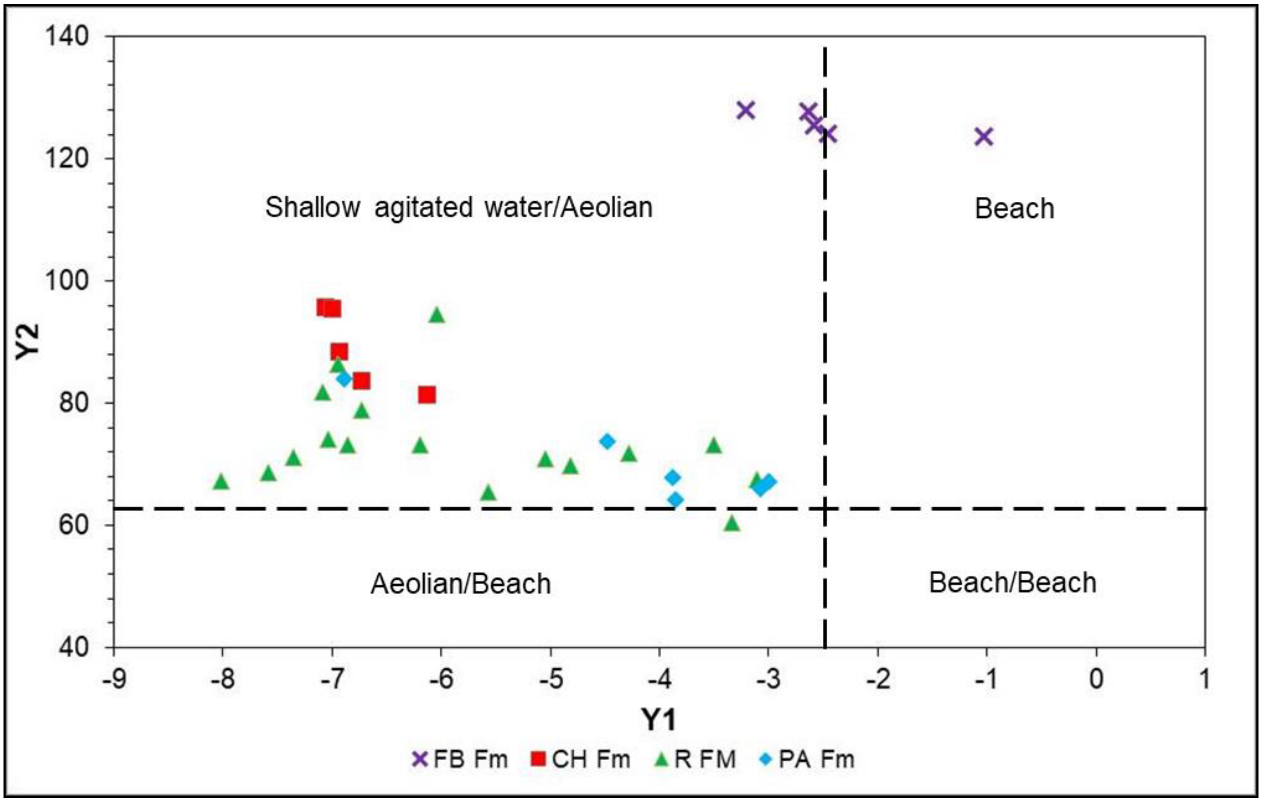

Figure 12. Linear discriminant function of Y2 versus Y1 displaying various depositional environments [30]

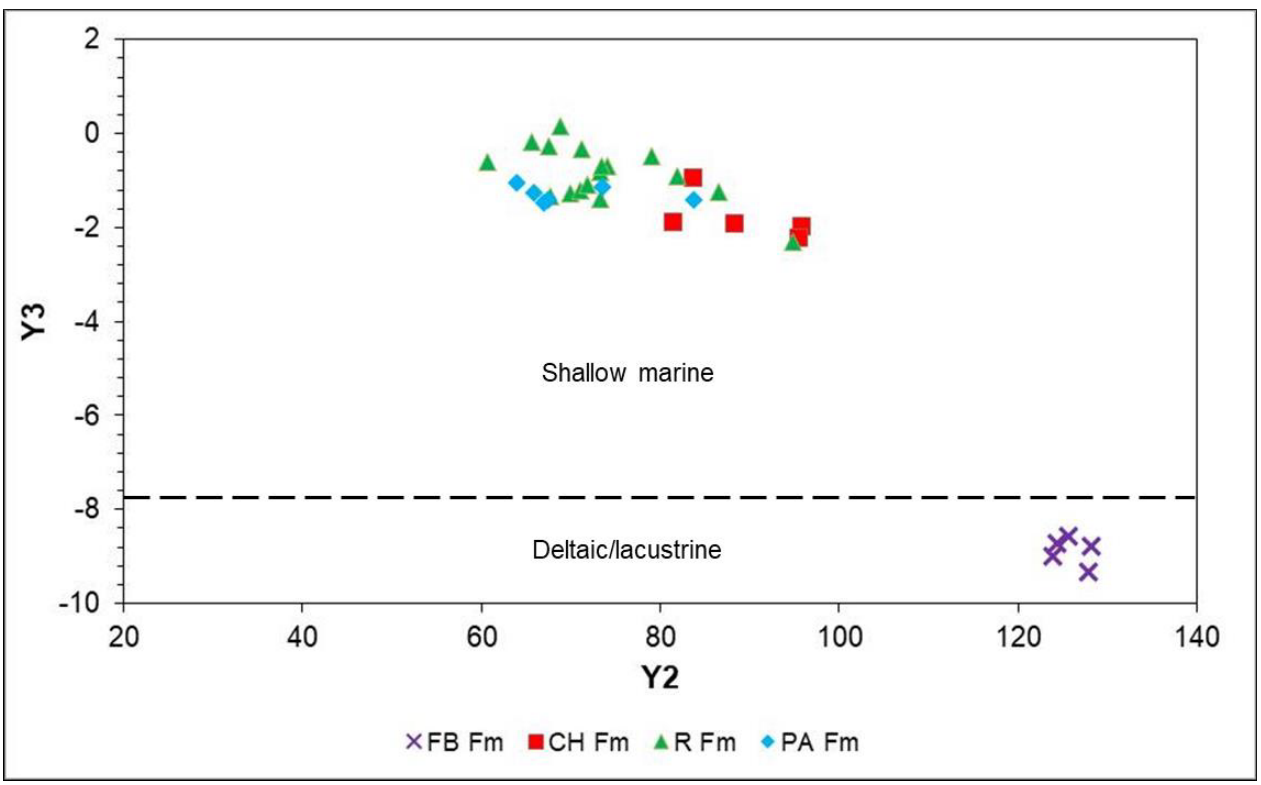

Figure 13. Linear discriminant function of Y3 versus Y2 displaying various depositional environments [30]

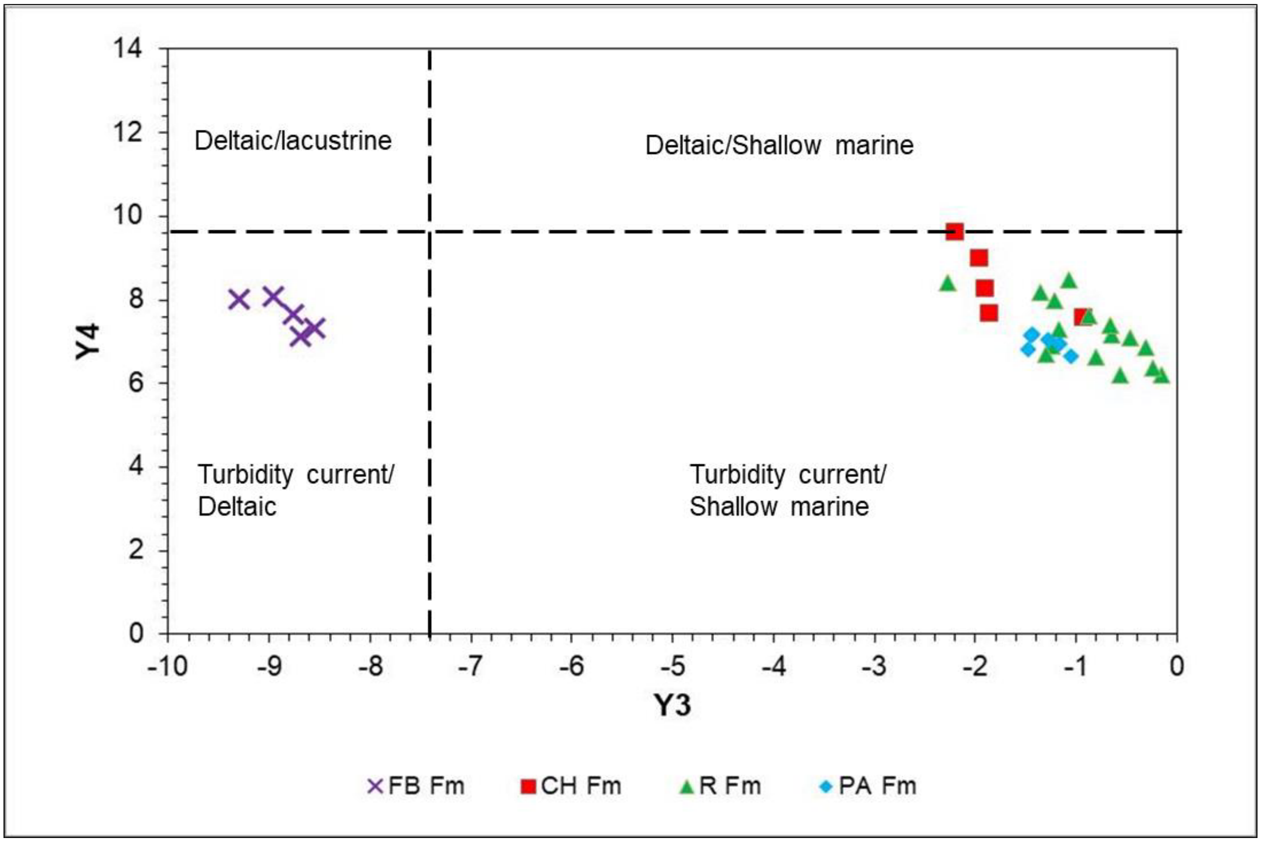

Figure 14. Linear discriminant function of Y4 versus Y3 displaying various depositional environments [30]

6. Conclusions

Grain size analysis was used to investigate and establish the transport mechanisms and depositional processes of sandstones from borehole KWV-1. To determine the depositional environment of the samples, grain size textural parameters such as mean, standard deviation, kurtosis and skewness were calculated. These parameters assisted in the construction of various plots, including the binary plots, linear discriminant functions, Passega diagrams (C-M pattern) and Visher diagrams. From analysing the grain sizes, the textural characteristics and depositional environments were derived. These sandstones are dominated by quartz and range in size from very fine-grained to fine-grained thus suggesting a generally low depositional energy. The main transportation mechanism is saltation for all the analysed samples with a few samples being transported through traction and suspension. From the linear discriminant diagram of Y1 versus Y2, all the samples were deposited in the shallow agitate waters and aeolian lacustrine. Y3 against Y2 functions indicate that deposition and sedimentation occurred in shallow marine waters. The Y3 versus Y4 plot indicates that the sandstones were a result of turbidity currents and deltaic processes.

References

[1] Boggs SJ. Petrology of sedimentary rocks, 2nd ed.; Cambridge University Press.; Cambridge, 2009; Chapter 2; p. 34.

[2] López GI. Grain size analysis. Encyclopedia of Geoarchaeology., November 2017, p. 341-348.

[3] Baiyegunhi C, Liu K, Gwavava O. Grain size statistics and depositional pattern of the Ecca Group sandstones, Karoo Supergroup in the Eastern Cape Province, South Africa. Open Geoscience. 2017; 9: 554-567.

[4] Baiyegunhi TL, Liu K, Gwavava O, Baiyegunhi C. Textural characteristics, mode of transportation and depositional environment of the Cretaceous sandstone in the Bredasdorp Basin, off the south coast of South Africa: Evidence from grain size analysis. Open Geosciences. 2020; 12: 1512-1532.

[5] Bull WB. Relation of textural (C-M) patterns to depositional environment of alluvial fan deposits. Journal of Sedimentary Petrology. 1962; 32 (2): 211-216.
[6] Angusamy NG, Rajamanikam V. Depositional environment of sediments along the southern coast of Tamil Nadu, India. Oceanologia. 2006; 1 (48): 87-102.
[7] Irudhayanathan A, Thirunavukkarasu R and Senapathi V. Grain size characteristics of the Coleroon Estuary sediments, Tamilnadu, East Coast of India. Carpathian Journal of Earth and Environmental Sciences. 2011; 6 (2): 151-157.
[8] Bumby A and Guiraud R. The geodynamic setting of the Phanerozoic basins of Africa. Journal of African Earth Sciences. 2005; 43 (1-3): 1-12.
[9] Smith RMH, Eriksson PG, Botha WJ. A review of the stratigraphy and sedimentary environments of the Karoo-aged basins of Southern Africa. Journal of African Earth Science. 1993; 16: 143-169.
[10] de Kock M, Beukes NJ, Adeniyi EO, Cole D, Götz AE, Geel C and Ossa F. Deflating the shale gas potential of South Africa's Main Karoo Basin. African Journal of Science. 2017; 113 (9): 1-12.
[11] Johnson MR, Van Vuuren CJ, Visser JNJ, Cole DI, de Wickens HV, Christie ADM and Roberts DL. The Foreland Karoo Basin, South Africa.; Amsterdam, Elsevier Science: Amsterdam, 1997; Vol.3, Chapter 12; p. 269-317.
[12] Linol B, Chere N, Muedi T, Nengovhela V and de Wit, MJ. Deep Borehole Lithostratigraphy and Basin Structure of the Southern Karoo Basin Re-visited. Regional Geology Reviews., September 2016, p. 101-108.
[13] Nolte S, Geel C, Amann-Hildenbrand A, Krooss BM and Littke R. Petrophysical and geochemical characteristics of potential unconventional gas shale reservoirs in the southern Karoo Basin, South Africa. International Journal of Coal Geology. 2019; 212 (103249):1-16.
[14] Baiyegunhi C and Liu K. Sedimentary facies, stratigraphy, and depositional environments of the Ecca Group, Karoo Supergroup in the Eastern Cape Province of South Africa. Open Geosciences. 2021; 13: 748-781.
[15] Galerne CY, Neumann ER and Planke S. Emplacement mechanisms of sill complexes: Information from the geochemical architecture of the Golden Valley Sill Complex, South Africa. Journal of Volcanology and Geothermal Research. 2008; 177: 425-440.
[16] Viglietti PA, Rubidge BS and Smith RMH. New Late Permian tectonic model for South Africa's Karoo Basin: Foreland tectonics and climate change before the end-Permian crisis. Scientific Reports. 2017; 7 (10861): 1-7.
[17] Woodford AC, Chevallier L, Botha JF, Cole D, Johnson MR, Meyer R, Simonic M, Van Tonder GJ and Verhagen B. Hydrogeology of the Main Karoo Basin: Current Knowledge and Future Research Needs. Water Research Commission. 2002; T 179/02:10-37, 49-50.
[18] Catuneanu O, Wopfner H, Eriksson PG, Cairncross B, Rubidge BS and Smith RMH. The Karoo Basins of south-central Africa. Journal of African Earth Sciences. 2005; 43: 211-253.
[19] Linol B and de Wit MJ. Origin and Evolution of the Cape Mountains and Karoo Basin. (Regional Geology Reviews), 1st ed.; Springer International Publishing.; Switzerland, 2016; Chapter 2; p.36-37.
[20] Campbell SA, Mielke P and Götz AE. Geothermal energy from the Main Karoo Basin: New insights from borehole KWV-1 (Eastern Cape, South Africa). Geothermal Energy. 2016; 4(9): 1-6.
[21] Geel C, Schulz HM, Booth P, de Wit M and Horsfield B. Shale gas characteristics of the Permian black shales in South Africa: Results from recent drilling in the Ecca Group, Eastern Cape. Energy Procedia. 2013; 40: 256-265.
[22] Catuneanu O, Hancox PJ and Rubidge BS. Reciprocal flexural behaviour and contrasting stratigraphies: a new basin development model for the Karoo retro arc foreland system, South Africa. Basic Research. 1998; 10: 417-439.
[23] Johnson MR, Anhaeusser CR and Thomas RJ. The geology of South Africa, 2nd ed.; Geology Society of South Africa.; Council of Geoscience.; Johannesberg, 2006; p. 461-499.
[24] Liu KW and Greyling EH. Grain size distribution and cementation of the Cretaceous Mbaza Formation of Eastern Cape, South Africa: A case study of a storm influenced offshore sequence. Sedimentary Geology. 1996; 107: 83-97.
[25] Johnson MR. Thin section grain size analysis revisited. Sedimentology. 1994; 41: 985-999.
[26] Wentworth CK. A scale of computing mechanical composition types in sediments. Geological Society of America Bulletin. 1992; 40: 760-771.
[27] Udden JA. Mechanical composition of clastic sediments. Geological Society of America Bulletin. 1914; 25: 655-744.

[28] Folk RL and Ward W. Brazos river bar: a study in the significance of grainsize parameters. Journal of sedimentary Petrology. 1957; 27: 3-26.
[29] Folk RL. Petrology of sedimentary rocks.; Hemphill Publishing Company.; Austin: Texas, 1974; Chapter 4; p. 41-45.
[30] Sahu BK. Depositional mechanism from the size analysis of elastic sediments. Journal of Sedimentary Petrology. 1964; 34(1): 73-83.
[31] Rajesh E, Anbarasu K and Rajamanickam GV. Grain size distribution of silica sand in and around Marakkanam coast of Tamil Nadu. Journal of the Geological Society of India. 2007; 69: 1361-1368.
[32] Ramanathan AL, Rajkumar K, Majumdar J, Singh G, Behera PN, Sandra SC, and Chidambaram S. Textural characteristics of the surface sediments of a tropical mangrove Sundarban ecosystem, India. Indian Journal of Marine Sciences. 2009; 38(4): 397-403.
[33] Selvaraj K and Ram Mohan V. Textural Variation and Depositional Environments of Inner shelf sediments, off Kalpakkam, Southeast Coast of India. Journal of the Geological Society of India. 2003; 61: 449-462.
[34] Martins LR. Recent sediments and grain size analysis. Gravel. 2003; 1: 90-105.
[35] Srivastava AK and Mankar RS. Grain Size Analysis and Depositional Pattern of Upper Gondwana Sediments (Early Cretaceous) of Salbardi Area, Districts Amravati, Maharashtra and Betul, Madhya Pradesh. Journal of the Geological Society of India. 2009; 73: 393-406.
[36] Moiola RJ and Weiser D. Textural parameters: an evaluation. Journal of Sedimentary Petrology. 1968; 38: 45-53.
[37] Rajganapathi VC, Jitheshkumar N, Sundararajan M, Bhat KH and Velusamy S. Grain size analysis and characterization of sedimentary environment along Thiruchendur coast, Tamilnadu, India. Arab Journal of Geoscience. 2013; 6: 4717-4728.
[38] Steward HB. Sedimentary reflection on depositional environment, in San Mignel lagoon, Baju California, Mexico. AAPG Bulletin. 1958; 42: 2567-2618.
[39] Friedman GM. Distinction between dune, beach and river sands from their textural characteristics. Journal of Sedimentary Petrology. 1961; 31: 514-529.
[40] Visher GS. Grain size distributions and depositional processes. Journal of Sedimentary Petrology. 1969; 39: 1074-1106.
[41] Singh BP. Sediment Dispersal Pattern in the Murree Group of the Jammu area, NW Himalaya, India. Himalayan Geology. 2000; 21 (1&2): 189-200.
[42] Passega R. Texture as characteristics of clastic depositional. American Association of Petroleum Geologists Bulletin. 1957; 41: 1952-1984.
[43] Passega R. Grain size representation by C-M pattern as a geological tool. Journal of Sedimentary Petrology. 1964; 34: 830-870.
[44] Chima P and Baiyegunhi C. Textural characteristics, mode of transportation and depositional environment of the Stormberg Group in the Eastern Cape. Geologos. 2022; 28(1): 61-78.

To whom correspondence should be addressed: Mahlatse M Ntake, Department of Geology and Mining, University of Limpopo, Private Bag X1106, Sovenga 0727, Limpopo Province, South Africa;
e-mail: manthepengntake@gmail.com